FIELD DETERMINATION OF BRAKING RATIOS FOR CARS IN COAL SERVICE

A STUDY OF BRAKING RATIO CHANGES FOR CERTAIN OLDER COAL CARS AND A NEW WAY TO DETERMINE BRAKING RATIO IN THE FIELD

For Presentation at the 91st Annual Technical Conference of the Air Brake Association, Chicago, IL, September 21, 1999

BY:

Cameron Lonsdale
Technical Manager-Railway Products
Standard Steel
Burnham, PA

Samuel Luke
Engineer of Freight Cars
Formerly with Conrail
Hollidaysburg, PA

Mark Lowe
Applications and Test Group Manager
Tekscan, Inc.
Boston, MA

James G. Rees
Managing Director
Interswiss, Ltd.
Chicago, IL

A STUDY OF BRAKING RATIO CHANGES FOR CERTAIN OLDER COAL CARS AND A NEW WAY TO DETERMINE BRAKING RATIO IN THE FIELD

Cameron Lonsdale
Technical Manager-Railway Products
Standard Steel
Burnham, PA

Mark Lowe
Applications and Test Group Manager
Tekscan, Inc.
Boston, MA

Samuel Luke
Engineer of Freight Cars
Formerly with Conrail
Hollidaysburg, PA

James G. Rees
Managing Director
Interswiss, Ltd.
Chicago, IL

ABSTRACT

Railroad cars in coal service in the northeastern United States are often shopped for wheel defects such as slid flat, built up tread and spalling. Previous work found that these defects can be caused by wheel sliding after air pressure leaks through defective service and emergency brake valve portions into the brake cylinder. Another important factor in the creation of wheel defects from wheel sliding is the car's empty braking ratio. If a car is excessively braked when empty, or has lost weight, there will be a greater chance for wheel sliding and damage. Wheel changeout data for different car classes were reviewed and several coal cars in the classes with the most wheel repairs were selected for detailed testing. The cars were given a complete air brake test, including a brake cylinder pressure test, and the brake system and wheels of each car was inspected. A static brake shoe force test was then conducted on each car in order to determine the current empty braking ratio, loaded braking ratio and hand braking ratio. A second set of static brake shoe force tests was also conducted using a new device that does not require removal of brake shoes and the results were compared to the first method. The potential use of the new brake shoe force test method as a field diagnostic tool to find cars with a high empty braking ratio is discussed, along with the need to find such cars in order to prevent excessive wheel changeouts. The potential use of the new method to check handbrake safety in the field is also discussed.

INTRODUCTION AND BACKGROUND

North American railroads removed over 129,000 railroad wheels during 1997 due to brake related wheel defects such as shelling (why made code 75), slid flat wheels (why made code 78) and built up tread (why made code 76) (Ref. 1). This represents a huge car maintenance cost for carriers and private car owners. Shelling, in most cases actually spalling, accounted for nearly 90,000 of the wheel removals and one recent paper estimated that this defect costs railroads $150,000,000 per year (Ref. 2). Removals for slid flat and built up tread wheels numbered 28,639 and 10,818, respectively, in 1997. In addition to the high costs of material, labor and time related to replacement of defective wheels, such wheel defects lead to increased damage to wheels, bearings, the track structure, lading and other freight car components. If methods are developed to reduce the incidence of these defects in service, rail carriers could invest scarce capital in other improvements.

Wheel shelling is considered condemnable in service if the defect "is 3/4 inch in length and in width or larger and the shells or spalls are more or less continuous around the periphery of the wheel or whenever any shell or spall is 1 inch or more in length and in width..." (Ref. 3). True wheel shelling is a mechanical rolling contact fatigue phenomenon and has been described in several papers (Ref. 4, 5, 6). However, most wheel shelling in North America is actually spalling which is related to sliding of the wheel on the rail. When sliding occurs, the steel at the wheel/rail contact patch is briefly austenitized due to frictional heating, and the colder body of the wheel then quenches the patch. A small patch of brittle, untempered martensite, with a slightly larger volume than the parent pearlitic wheel steel, results and this leads to eventual cracking and spalling of steel off the wheel tread under service loading. Numerous papers have described wheel spalling in great detail, and some are referenced here (Ref. 7, 8, 9, 10).

Tread slid flat wheel defects are condemnable if the defects are two inches or more in length or have two or more adjoining spots each 1-1/2 inch or more in length (Ref. 3). Such defects are considered to be the responsibility of the "handling line." Built up tread wheel defects are considered condemnable if the tread has built up metal 1/8 inch or higher than the wheel tread (Ref. 3). Both defect types are known to cause severe impact loads between the wheel and rail in service and have also caused derailments.

PREVIOUS INVESTIGATIONS - BRAKE RELATED WHEEL DEFECTS

There have been a number of studies designed to identify the root cause of brake related wheel defects such as spalling, built up tread and slid flat wheels, and a few studies will be discussed here. Carmean and Butler linked abnormally high brake cylinder pressure caused by defective service and emergency portion "o" rings to built up tread and slid flat wheel defects in a 1996 paper delivered to the Air Brake Association (Ref. 11). The work of these authors contributed to the adoption of brake cylinder pressure testing by the

Association of American Railroads. At the 1997 Air Brake Association meeting, Janshego and Lonsdale suggested that wheel shelling (spalling) on coal cars was also linked to the same air brake system defect (Ref. 12).

Further work during 1998 by Butler, Lonsdale and Luke revealed that abnormally high brake cylinder pressure was closely linked to built up tread, slid flats and wheel spalling (Ref. 13) on cars in coal service. High brake cylinder pressure was found for 80% of the cars with built up tread, 72% of the cars with slid flats and 38% of the cars with wheel shelling/spalling. These authors also performed a series of static dynamometer brake force tests on a group of coal cars with repeat wheel changeouts to determine the "current" empty braking ratio of the cars. It was found that the cars had lost considerable weight (assumed to be due to corrosion) during their time in service (20-25 years) and that the "current" empty braking ratio had increased from the "as built" value in every case. Some of the cars were above the AAR specified value for new car empty braking ratio. This condition would lead to easier sliding of wheels on an empty car and would lead to additional wheel damage in service.

Blevins reported that Canadian National's (CN) wheel shelling (spalling) problems were strongly related to wheel sliding caused by movement of cars with the hand brakes applied (Ref. 14). CN found evidence that martensite patches caused by hand brake wheel sliding led to further cracking and spalling under in service loads. The tread cracking was later exacerbated by water from blowing snow that filled the cracks. Another paper by AAR researchers examined the effects of brake-beam guide-slot liners and empty/load devices on wheel sliding (Ref. 15). This work found that improved empty/load devices have the potential to reduce the incidence of wheel spalling and that steel or a new type polymer brake beam guide slot liner may have a similar benefit.

Bartley of Canadian Pacific (CP) presented data suggesting that the rate of shelling is inversely related to empty car weight (Ref. 16). These data showed that the less a car weighed, the greater percentage of wheels removed for shelling. Bartley also offered CP's experience that a lower braking force in relation to car weight results in a reduced incidence of shelling for non-steered equipment.

WHEEL SLIDING AND BRAKING RATIO

A wheel will slide on a rail when the retarding force of brake shoe on wheel tread (a function of braking force x friction) is greater than the force between wheel and rail (Ref. 17). If the force between wheel and rail is reduced because the car is empty, the chance for wheel sliding increases. Likewise, if a car has lost weight due to corrosion, the opportunity for wheel slip will tend to increase. Other factors affecting adhesion include wheel/rail profiles, rail surface condition, etc.

Braking ratio is defined as the ratio of brake shoe force against the wheels to the car's weight (Ref. 17). In the case of an empty car, the braking ratio is described as a percentage of the car's light weight. However, for the hand braking ratio and loaded net braking ratio, the value is a percentage of the car's gross rail load (GRL). These values must be determined for each type of car when the car is constructed. Current AAR Standards require freight cars (except TOFC/COFC cars) to have to have a loaded braking ratio (with high friction composition shoes) between 8.5% and 13% of GRL, a minimum hand braking ratio which is 10% of GRL, and a maximum empty braking ratio of 38% (Ref. 18). These braking ratio values are calculated using brake shoe forces measured given a 30 psi brake pipe reduction from 90 psi brake pipe pressure.

SELECTION OF CARS FOR TESTING

Wheel repeat changeout data (1992-1996) for Conrail owned coal cars with why made codes 67 (wheel out-of-round), 75 (shelling), 76 (tread built up) and 78 (tread slid flat) were examined to find candidate car classes for braking ratio determination. Data were based upon repeat wheelset changes by position on a given car. For example, if a wheelset on a car was changed for R1 and later for R1 or L1, it would count as a repeat. However, if each of the four wheelsets were changed without repeating position (e.g.: R1, then L3, then L2), the car was not identified as a repeater. Wheel changeout data are shown in Table 1.

Car Class	Class Average Age*	Total Number Cars In Class*	Number Repeat Cars In Class	Number Why Made 67	Number Why Made 75	Number Why Made 76	Number Why Made 78	Total Of 4 Why Made Codes
HR1A	31.2	67	2	0	4	0	14	**18**
HR1C	36.2	147	3	0	3	7	12	**22**
H1A	19.7	475	12	0	7	38	23	**68**
H1B	19.7	2,678	78	9	113	175	242	**539**
H1C	19.5	973	19	1	29	27	32	**89**
H1D	19.3	155	2	0	0	16	4	**20**
H1E	18.7	498	17	1	13	67	54	**135**
H1G	19.3	523	12	0	9	35	38	**82**
H1L	24.5	270	4	1	2	3	33	**39**
H43	33.9	160	3	0	0	0	20	**20**
H43A	33.0	76	2	0	0	14	40	**54**
H43B	32.6	151	4	0	7	6	29	**42**
H43C	31.3	41	1	0	2	0	0	**2**
H43D	26.3	200	3	0	2	4	6	**12**
	Total	**6,414**	**162**	**12**	**191**	**392**	**547**	**1,142**

Note: *Age/number data current as of 5/18/98.

Table 1. Conrail coal car repeat wheel changeout data.

Based upon the data in Table 1 it was decided to test cars from the H1B, H1C and H1E classes. These three car classes had the highest numbers of repeat wheel defects. Rather than attempt to select specific H1B and H1C cars from the repeat list and have those cars found, switched out and shopped for detailed testing, 4 cars were selected at random from coal cars stored awaiting major repairs at Conrail's Shire Oaks, PA, yard. The 4 cars, which were selected and weighed at Shire Oaks by Conrail Mechanical

Department personnel, are CR 488996 (H1B), CR 490254 (H1C), CR 487881 (H1B), and CR 488060 (H1B). The advantage of such a random selection process was that the cars were readily available. However, none of these cars were on the repeat wheelset changeout list. Each car was then given an air brake test, including the brake cylinder leakage test, to determine if there were any abnormalities with the brake system. Static brake force dynamometer testing was then scheduled for February, 1999, at the Shire Oaks Car Shop.

TEST METHODOLOGY

First, the current empty braking ratio, loaded braking ratio and hand braking ratio of each car would be determined using the Jim Shoe® static dynamometer brake shoe test device. This would allow us to see if current braking ratio values met AAR standards for new cars. Secondly, the test work would compare the force values obtained using the Jim Shoe® and results obtained using the newly developed "Membrain®" static dynamometer brake shoe force test device. The new device, which does not require removal of brake shoes to obtain shoe force values and therefore is easier to use, could be of great benefit to field railroad car shops in determining the current suitability of a car's brake system for service. It was hoped that important information on freight car safety and wheel defect causes could be obtained while development work on the new brake shoe force measuring device continued.

BRAKING RATIO RESULTS USING JIM SHOEÒ

Static dynamometer brake shoe testing results for the 4 selected coal cars are shown in Table 2. Braking ratio data are shown as a percentage throughout the paper.

Car Number	Original Lt. Weight (lb.)	Present Lt. Weight (lb.)	Weight Loss (lb.)	Curr. Empty Brake %	Curr.Load Brake %	Curr. Hand Brake %
CR 488996	59,200	54,000	5,200	35.1	7.2	11.3
CR 490254	58,500	55,200	3,300	35.2	7.4	13.2
CR 488060	59,200	52,700	6,500	30.9	6.2	8.8
CR 487881	59,200	53,700	5,500	32.5	6.6	Not Tested

Table 2. Braking ratio results using Jim ShoeÒ device.

The results show that all of the cars currently have a loaded braking ratio below the AAR requirement for newly constructed cars. Further, CR 488060 does not have the required amount of hand braking ratio for a newly constructed car. Also note that CR 488996 and CR 490254 are within 3% of the maximum allowable empty braking ratio for a newly constructed car. During periods of low adhesion during empty braking, these cars will have a greater likelihood of wheel sliding and damage. Finally, the large amount of weight loss for each of the cars listed in Table 2 is somewhat surprising. The average amount of weight lost by the four cars is 5,125 pounds.

Air brake system diagnostic testing prior to the static dynamometer brake force tests found that each car needed at least one new brake valve portion. Shop personnel reported that CR 488996, CR 490254 and CR 488060 all needed new service portions, while CR

487881 needed both a new service portion and an emergency portion. Maintenance records show that three of the cars had emergency portion repairs performed within the last few years, as follows: CR 488996 (2/96), CR 488060 (9/95) and CR 487881 (5/93). The number of recorded wheel repairs for the cars was not excessive, and the tread condition of wheels at the time of testing was fairly good. There was evidence of spalling and wheel sliding on some wheels, however. On a qualitative basis, the wheel treads on CR 488060 appeared to be in the worst condition.

DECSRIPTION OF NEW BRAKE SHOE FORCE SENSOR TECHNOLOGY

The brake shoe force sensor technology (Pressure Measurement System) developed by Tekscan encompasses four distinct areas: sensor technology, data acquisition hardware, processing and analysis software, and materials technology (Ref. 19). Each of these areas has a number of patents, copyrights or patents pending supporting Tekscan's intellectual property claims. Packaging designs adapting the sensors to rail car applications are being developed as proprietary designs by Interswiss, Ltd., who will be cooperating in the development of application engineering and will be marketing the finished products for brake force measurement and evaluation.

Sensor Technology

The Pressure Measurement System utilizes an extremely thin (~0.1 mm), flexible tactile force sensor. These sensors are capable of measuring pressures ranging from 0 to 175 MPa. Each application requires an optimal match between the dimensional characteristics of the object(s) to be tested and the spatial resolution and pressure range provided by the sensor technology. Sensing locations within a matrix can be as small as 0.0009 in.^{2} (0.140 mm^2) and therefore, a 1 cm^2 area can contain an array of 170 sensing locations. The pressure or force information derived from the sensor array is then displayed on the computer screen.

The standard sensor consists of two thin, flexible polyester sheets which have electrically conductive electrodes deposited in varying patterns. In the simplified example shown in Figure 1 on the following page, the inside surface of one sheet forms a row pattern while the inner surface of the other employs a column pattern. The spacing between the rows and columns varies according to sensor application and can be as small as ~0.5 mm. Before assembly, a patented, thin, semi-conductive coating (ink) is applied as an intermediate layer between the electrical contacts (rows and columns). This ink, unique to sensors produced by Tekscan, provides the electrical resistance change at each of the intersecting points.

When the two polyester sheets are placed on top of each other, a grid pattern is formed, thus creating a sensing location at each intersection. By measuring the

Figure 1. Schematic of Pressure Measurement

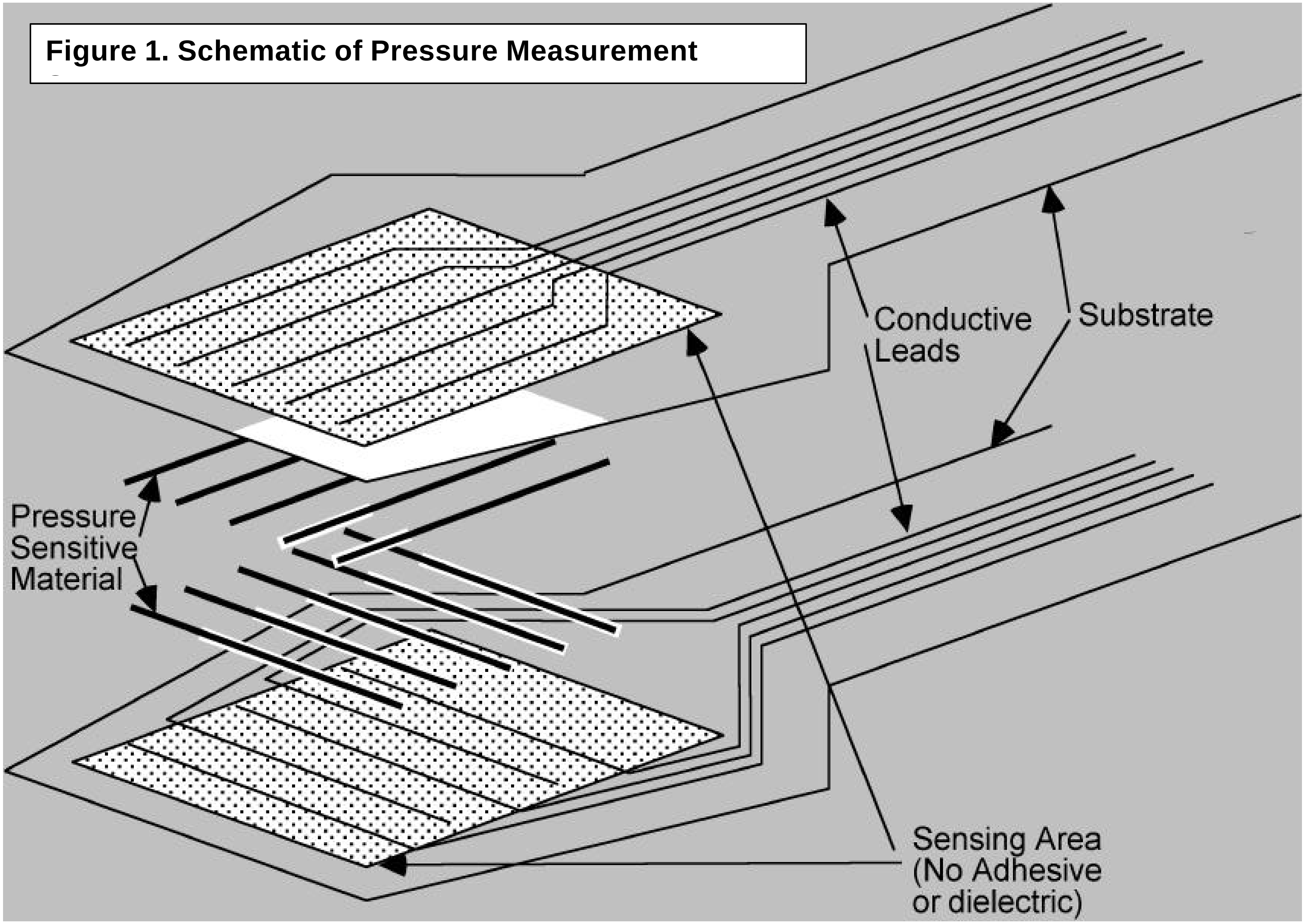

changes in current flow at each intersection point, the applied force distribution pattern can be measured and displayed on the computer screen. With this system, force measurements can be made either statically or dynamically and the information can be seen as graphical, informative 2-D or 3-D displays. In use, the sensor is installed between two mating surfaces. Tekscan's matrix-based systems provide an array of force sensitive cells that enable the user to measure the pressure distribution between the two surfaces. The 2-D and 3-D displays show the location and magnitude of forces exerted on the sensor surface at each sensing location. Force and pressure changes can be observed, measured, recorded, and analyzed throughout testing.

Data Acquisition, Display, and Analysis Software

The system functions in both static and dynamic measurement environments. Temporal development of load profiles and peak load attainment can be measured, as well as the relaxation characteristics of materials. Each system is capable of sampling thousands of sensors per second and the standard I-Scan system can sample 250,000 sensors per second. Custom data acquisition hardware and Windows™ compatible software make this possible.

Real time 2-D color displays and 3-D wire frames are clear and easy to use. The software enables the user to view a cross-sectional presentation, locate areas of interest, and display temporal, force, and pressure characteristics on-screen. Various plots of force, pressure, and time are available. Basic mathematical operations, such as peak pressure distribution, average, minimum, maximum, and center of force, and many more, are also available.

Data Acquisition Hardware

A variety of data acquisition interfaces, ranging from the simple serial board to more complex parallel and ISA interface boards, are available. The brake force measurement system uses sophisticated microprocessor-based circuitry to control scanning, adjust sensitivity and optimize performance. The sensing system scans the intersecting points of the sensor's rows and columns and measures the resistance at each contact point. These points are read in the presence of multiple contacts, while simultaneously limiting the possible current flow through the device. A variable resistor represents each contact location, and these resistors have a high value when no force is applied to them. The brake force sensing system is controlled using a personal computer and software and each sensor is read sequentially by driving one of the rows and sensing one of the columns. The microprocessor selects the row and column to be read by identifying the proper address for each intersecting row and column.

RESULTS AND DISCUSSION

The data taken from the three rail cars during the air brake tests are shown in Table 3. These data show a comparison of brake shoe force measured using the currently available

Jim Shoe® static dynamometer brake shoe force test device (Ref. 20) and the new Membrain® device. The total (sum) brake shoe force values correlate fairly well considering that some force variation can occur each time a car's brakes are applied. The smallest percent difference between the total brake shoe force as reported by the Jim Shoe® and the Membrain® is approximately 3% while the largest difference is approximately 11%. However the standard deviation of the Membrain® data from wheel to wheel is greater than the Jim Shoe® data. Finally, take note of the large variations in brake shoe force from wheel to wheel, axle to axle and car to car.

	Rail Car #1 - CR 488996			Rail Car #2 - CR 490254			Rail Car #3 - CR 488060		
Wheel Loc.	Membrain (pounds)	JimShoe (pounds)	% diff.	Membrain (pounds)	JimShoe (pounds)	% diff.	Membrain (pounds)	JimShoe (pounds)	% diff.
L1	2,756	2,129	-29.45	2,622	2,178	-20.39	1,263	1,663	24.05
L2	2,647	2,221	-19.18	2,289	2,474	7.48	1,560	2,016	22.62
L3	2,393	2,185	-9.52	1,971	2,021	2.47	2,274	1,913	-18.87
L4	2,721	2,788	2.40	2,779	2,607	-6.60	2,029	2,366	14.24
R1	2,796	2,480	-12.74	2,194	2,776	20.97	1,409	2,034	30.73
R2	2,019	2,424	16.71	2,428	2,743	11.48	1,565	2,024	22.68
R3	2,394	2,282	-4.91	1,975	2,180	9.40	2,423	2,126	-13.97
R4	1,734	2,435	28.79	2,000	2,434	17.83	1,945	2,139	9.07
Total	19,460	18,944	-2.7%	18,258	19,413	6.0%	14,468	16,281	11.1%
S.dev.	358	199	--	288	261	--	394	188	--

Table 3. Air brake comparison testing.

The data taken from the three rail cars during the hand brake tests are shown in Table 4. The total braking force values do not correlate well between the Jim Shoe® tests and the Membrain® tests. The data from the Membrain® are substantially lower than the data from the Jim Shoe® and vary from a 15% difference to a 27% difference. The standard deviations from these data are larger than those from the air brake tests and the Membrain® data shows a higher standard deviation on two of the three cars.

	Rail Car #1 - CR 488996			Rail Car #2 - CR 490254			Rail Car #3 - CR 488060		
Wheel Loc.	Membrain (pounds)	JimShoe (pounds)	% diff.	Membrain (pounds)	JimShoe (pounds)	% diff.	Membrain (pounds)	JimShoe (pounds)	% diff.
L1	3,875	3,925	1.27	4,202	4,976	15.55	1,639	2,512	34.75
L2	3,739	3,689	-1.36	3,659	4,517	18.99	2,300	2,999	23.31
L3	2,654	3,077	13.75	2,817	3,175	11.28	2,191	2,755	20.47
L4	3,433	3,770	8.94	4,114	4,473	8.03	2,050	3,121	34.32
R1	4,135	4,322	4.33	3,931	5,620	30.05	2,012	2,965	32.14
R2	2,681	4,342	38.25	4,108	4,856	15.40	2,053	2,914	29.55
R3	2,638	3,212	17.87	2,714	3,241	16.26	2,618	3,122	16.14
R4	2,072	3,367	38.46	2,933	3,895	24.70	2,003	2,820	28.97
Total	25,227	29,704	15.1%	28,478	34,753	18.1%	16,866	23,208	27.3%
S.dev.	690	446	--	595	800	--	262	190	--

Table 4. Hand brake comparison testing.

There are many reasons why the data collected with the two force measurement systems show a difference. The electronics, sensor, calibration and the packaging of the sensor of the Membrain® system were not optimal for the field test since the device was under development. Additionally, since the test data from the Jim Shoe® and the Membrain® system were not collected concurrently, the results from the tests are not a direct force comparison. We assumed that resultant brake shoe force values were repeatable from brake application to application. However, since the Jim Shoe® and Membrain® data were not obtained during the same air brake application, variation in brake shoe force due to other variables (levers, shoe alignment, etc.) could have resulted in unwanted variation in the comparison data.

The data obtained in these tests were subject to conditions that were not conducive to the greatest accuracy. The harsh environment between brake shoes and wheels is not optimal for producing laboratory grade results. The Membrain® devices used in the tests were improvised rather quickly to meet the time schedule of the tests. Due to the surface irregularities of the mating parts, direct exposure of the electronic sensors to the brake shoe and wheel tread surfaces was not feasible since there was the possibility of damaging the sensor surfaces. It was therefore necessary to devise packaging for the devices to protect them from damaging conditions.

The taper of the wheel tread causes a non-normal force component that must be taken into account algebraically and also causes certain mechanical problems. A sort of “sandwich” arrangement was developed for the Membrain® sensor device to deal with this situation. Stainless steel shim stock 0.012 in. thick was cut to the approximate dimensions of the resistor grid array. A thin film of silicon “O ring” lubricant was applied to the mating surfaces of the shim-sensor surfaces to prevent damaging shear forces caused by the taper, and the sub-assembly was then placed between two layers of 0.031 in. thick polyurethane sheets. The sheets were not bonded into a coherent assembly because of time constraints as well as the uncertainty inherent with new experimentation.

Some relative motion between the parts was inevitable and undesired, since the wheel tread taper produced sliding forces and the parts were not rigidly connected. Future assemblies will follow more along the lines of an assembly that is designed to overcome these problems and also protect the parts from damage. Improved accuracy is expected as a result. An interim design is shown as Figure 2 on the following page. The area at the lower left in Figure 2 is an electrical connector while the horizontal section is placed between the brake shoe and wheel tread. Further experimentation is expected to yield an improved, coherent design that is more accurate and easier to use.

The Membrain® system electronics has an 8 bit dynamic range for each sensel. This means that the device can digitize an analog signal into 256 individual (digital) values. The mean digital output value from the sensels during field testing was approximately 20 and 23 for the handbrake tests. Therefore, less than 10% of the system’s dynamic range was used, and this can create errors in the reported values. Because each digital level represents 5% (or 1/20) of the mean, a small variation in the digital signal can lead to a large error in the measurement.

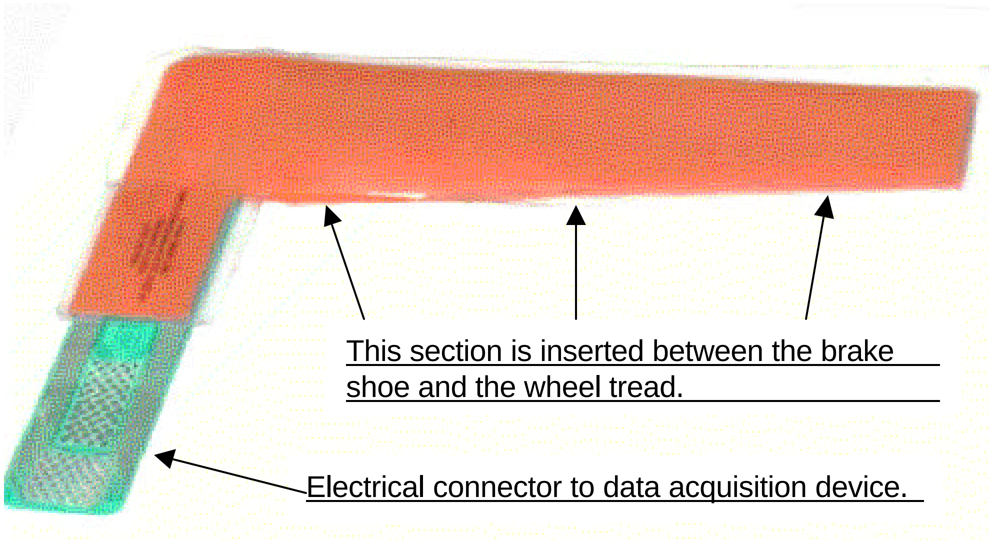

Figure 2. Photo showing interim Membrain® design.

The Membrain® sensors were previously calibrated at load levels of 1,000 pounds and 6,000 pounds. Data obtained from these two loading points were used to develop a power law (i.e. $y=a*x^b$) calibration equation for the Membrain®. This non-linear equation is used to account for the non-linear nature of the materials that are applying the load. The non-linear curve fit is typically more accurate at the two calibration points. The data from the airbrake test is closer to the 1,000 pounds calibration point than the data from the handbrake test. This may account for better data correlation during the air brake testing than during the hand brake tests.

Another problem was that since this was an experimental application, it was necessary to use an existing sensor that had been manufactured for a different purpose and did not dimensionally match the dimensions of the brake shoe. As a result, the brake shoe applies loads outside the useable sensing area, as shown in Figure 3. The right hand side of the figure shows a load pattern at the edge of the sensor. This load probably extends well beyond the measuring area thus causing the sensor to underreport the force actually imparted between the brake shoe and the wheel. The left-hand side of Figure 3 shows the outline of a “normal” brake shoe half.

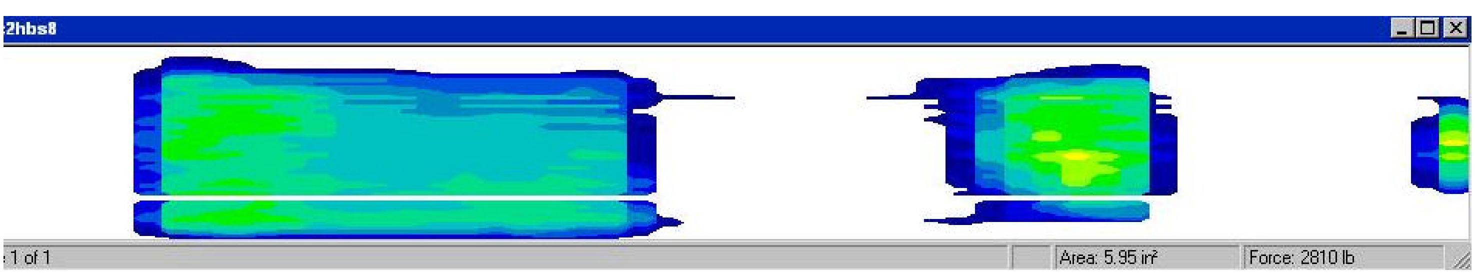

Figure 3. Force data outside the sensing area.

For the purpose of the field test, the Membrain® sensors were placed between two thin metal sheets to protect them from damage. Additionally, a 0.065 in. thick rubber strip was placed between the metal sheet and the sensor to control the contact area and load path of the brake shoe force. The area of the sensor where the rubber was placed was thicker than the remainder of the sensor and therefore as the two mating surfaces (brake shoe and wheel tread) where pushed together, the loading path should have been through the rubber. However, during the field tests the brake shoes deflected and made contact outside the thicker area as shown in Figure 3.

CONCLUDING REMARKS

Ideally the data from this type of comparative brake force field experiment should be collected concurrently. However, since the two force measuring devices cannot be tested on the same wheel during the same brake application, concurrent testing is not possible. Given all the possible sources of error, the data from these tests show the new device to be viable. After the Membrain® device has been made more robust for field testing and the issues of dynamic range, calibration and packaging are addressed, further testing should be performed.

The testing shows that the current braking ratios of a freight car can vary substantially from the braking ratio values required by the AAR for newly constructed cars. The empty braking ratio can affect the incidence and severity of wheel tread defects while the loaded braking ratio and hand braking ratio are clearly safety related issues. We suggest that further brake shoe force testing be performed on currently operating freight cars of various types, particularly for those cars with a history of repeat repairs for brake related wheel defects. Also, the issue of brake shoe force variations on a given car should be explored. Inefficiencies in the brake system can result in more force being applied on one wheel of an axle than another and this could lead to additional wheel tread damage.

REFERENCES

1. Association of American Railroads, Car Repair Billing Data, AAR, Pueblo, CO.

2. D. R. Hoffman, Presentation to the Car Department Officers' Association Annual Meeting, Chicago, IL, September 15, 1997.

3. AAR 1999 Field Manual of the Interchange Rules, Association of American Railroads, Washington, D. C., 1999.

4. J. Kalousek, J. H. Hornaday, Jr., and W. N. Caldwell, "Wheel Shelling Problems on the Canadian National Railways' British Columbia Northline," *Proceedings of the 9th International Wheelset Congress*, Montreal, PQ, Canada, 1988, Paper 5-2.

5. Eric Magel and Joe Kalousek, "Identifying and Interpreting Railway Wheel Defects,"

Proceedings of the International Conference on Freight Car Trucks/Bogies, Montreal, PQ, Canada, June 9-12, 1996, pp. 5.7-5.20.

6. E. Magel and J. Kalousek, "Martensite and Contact Fatigue Initiated Wheel Defects," *Proceedings of the 12th International Wheelset Congress*, Qingdao, China, September 21-25, 1998, pp. 100-111.

7. D. H. Stone, G. J. Moyar, and T. S. Guins, "An Interpretive Review of Railway Wheel Spalling and Shelling," ASME RTD Vol. 5, 1992, pp. 97-103.

8. H. C. Iwand, D. H. Stone, and G. J. Moyar, "A Thermal and Metallurgical Analysis of Martensite Formation and Tread Spalling During Wheel Skid," ASME RTD Vol. 5, 1992, pp. 105-116.

9. Kevin J. Sawley, "Railway Wheel Slide Damage," *Proceedings of the Engineering Against Fatigue Conference*, University of Sheffield, England, March, 1997.

10. Jian Sun et al., "Progress in the Reduction of Wheel Spalling," *Proceedings of the 12th International Wheelset Congress*, Qingdao, China, September 21-25, 1998, pp. 18-29.

11. Joe W. Carmean and Sam L. Butler, "Asset Optimization Through Train Air Brake Failure Analysis and Corrective Actions," Presentation to the Air Brake Association and Car Department Officers' Association, Chicago, IL, September 16, 1996.

12. S. W. Janshego, II and C. P. Lonsdale, "Conrail Use of Over-the-road Testing to Investigate the Cause of Wheel Shelling on Cars in Coal Service," *Proceedings of the 89th Annual Convention and Technical Conference of the Air Brake Association*, Chicago, IL, September 16, 1997, pp. 187-200.

13. S. L. Butler, C. P. Lonsdale and S. T. Luke, "Conrail Use of Brake Cylinder Pressure Testing to Investigate Brake Related Wheel Defects," Presentation to the Air Brake Association, Chicago, IL, September 16, 1998.

14. W. G. Blevins, "CN Wheel Spalling and Shelling," Presentation to the Air Brake Association, Chicago, IL, September 16, 1998.

15. Daniel H. Stone, Frederick G. Carlson, and Carl G. Bachhuber, "Effect of Brake-System Components on Wheel Spalling," ASME Winter Meeting, Anaheim, CA, November, 1998.

16. G. W. Bartley, "A Practical View of Wheel Tread Shelling," *Proceedings of the 9th International Wheelset Congress*, Montreal, PQ, Canada, 1988, Paper 5-1.

17. The Air Brake Association, *Management of Train Operation and Train Handling*, Chicago, IL, Air Brake Association, 1972.

18. Association of American Railroads, Standard S-401 Freight Car Brake Design Requirements, January 27, 1997.

19. Tekscan, Inc., Corporate Information, Unpublished report, 1999.

20. James G. Rees, “Brake Force Measurement,” Presentation to the Air Brake Association, Chicago, IL, September 22, 1980.